

Gravitational Baryogenesis in Hořava-Lifshitz gravity

Sayani Maity,^a Prabir Rudra ^{1b}

^a*Department of Mathematics, Techno India Salt Lake, Sector-V, Kolkata-700 091, India.*

^b*Department of Mathematics, Asutosh College, Kolkata-700 026, India.*

E-mail: sayani.maity88@gmail.com, prudra.math@gmail.com

ABSTRACT: In this work we intend to address the matter-antimatter asymmetry via the gravitational baryogenesis mechanism in the background of a quantum theory of gravity. We investigate this mechanism under the framework of Hořava-Lifshitz gravity. We will compute the baryon-to-entropy ratio in the chosen framework and investigate its physical viability against the observational bounds. We also conduct the above study for various sources of matter like scalar field and Chaplygin gas as specific examples. We speculate that quantum corrections from the background geometry will lead to interesting results.

KEYWORDS: Baryogenesis, Hořava-Lifshitz, Baryon, Entropy, scalar field, Chaplygin gas.

arXiv:1802.00313v2 [gr-qc] 2 Feb 2018

¹Corresponding Author

Contents

1	Introduction	1
2	Baryogenesis mechanism in the background of Hořava-Lifshitz Gravity	3
3	Baryogenesis with Scalar Field	7
4	Baryogenesis with Generalized Chaplygin Gas	8
5	Conclusion	12

1 Introduction

Cosmic Microwave Background observations [1] and Big Bang nucleosynthesis predictions [2] have confirmed the presence of excess matter over antimatter in the universe. There has been a lot of debate over such observations and gravitational baryogenesis have been proposed as the most suitable mechanism for such asymmetry [3–6]. Baryogenesis mechanism incorporates one of Sakharov’s criteria [7]. According to him in the process of generation of matter-antimatter asymmetry the following three conditions must be satisfied: baryon number non-conservation, C and CP symmetry violation and deviation from thermal equilibrium.

The baryon asymmetry gravitational baryogenesis term used in [3] is of the form

$$\frac{1}{M_*^2} \int d^4x \sqrt{-g} (\partial_\mu R) J^\mu, \quad (1.1)$$

where the parameter M_* is the cut-off scale of the underlying effective gravitational theory. J^μ , g and $R = 12H^2 + 6\dot{H}$ stand for the baryonic matter current, the trace of the metric tensor and the Ricci scalar respectively. This is a CP-violating interaction term which can be acquired from higher order interactions in the fundamental gravitational theory [3]. If flat FRW geometry is considered then baryon-to-entropy ratio η_B/s is proportional to \dot{R} . Further the baryon-to-entropy ratio becomes zero when the matter fluid corresponds to relativistic matter with EOS parameter $\omega = 1/3$. The predicted baryon-to-entropy ratio is $\eta_B/s \simeq 9.2 \times 10^{-11}$ [8].

With the discovery of the accelerated expansion of the universe [9, 10], Einstein’s theory of general relativity needed serious revisions and hence different dynamical dark energy models and modified theories of gravity came to the foreground. Moreover there has been a prolonged attempt to reconcile the physics of the large with the physics of the

small which will result in a quantum theory of gravity. Hořava-Lifshitz gravity is a novel attempt towards such a theory of quantum gravity [11–13]. The theory is devoid of full diffeomorphism invariance but it has UV completeness. Not only that, the theory has a three dimensional general covariance and time re-parameterization invariance. In fact it is a non-relativistic renormalizable quantum theory of gravity possessing higher order spatial derivatives [14, 15]. The singularity problem has plagued most of the basic theories of cosmology over the years. The singularity at the beginning of the universe and the singularity inside a black hole has remained a totally unknown and unexplained fact. One of the basic motivations of the Hořava-Lifshitz gravity is to provide an explanation to the singularity paradigm. Recently there have been extensive research in Hořava-Lifshitz gravity [16–20].

Various dark energy candidates have been proposed to explain the late time acceleration. The cosmological constant is the most common candidate that plays the role of dark energy. Various other models of dark energy have been proposed over the years without using the cosmological constant. There is one class of dynamical dark energy models which includes a scalar field [21, 22]. The introduction of the scalar field ϕ makes the vacuum energy dynamical and the model can represent a wide range of cosmological scenarios from inflation to late time acceleration. In the scalar field models ϕ is assumed to be spatially homogeneous, $\dot{\phi}^2/2$ is the kinetic energy and $V(\phi)$ is the potential energy [22]. Scalar field models of DE have been discussed in [23–26]. Chaplygin gas model [27, 28] is another form of dark energy proposed in literature. From the initially developed pure Chaplygin gas it gradually evolved to generalized Chaplygin gas (GCG). The GCG model has been discussed extensively in literature [29–34] as an effective model of dark energy for interpreting the accelerating universe. Interestingly, it describes two unknown dark sectors of the universe- dark energy and dark matter in a single matter component [35]. It is characterized by an exotic equation of state $p_{GCG} = -\frac{A}{\rho_{GCG}^\alpha}$, where $0 < \alpha \leq 1$ and A is a positive constant [36]. For $\alpha = 1$, it gives original Chaplygin gas and $\alpha = 0$ accounts for Λ CDM model. To constrain the parameter space, GCG model has been investigated with different cosmic observational data set such as the baryon acoustic oscillation (BAO), microwave background radiation (CMBR), geometric information from SN Ia [37–40].

Gravitational baryogenesis has been studied under the framework of different gravity theories over the past few years. In 2006 baryogenesis was investigated in the framework of $f(R)$ gravities in [4]. In [41] Ramos and Paramos generalized this model by introducing a non-minimal coupling (NMC) between curvature and matter and investigated the impact of NMC on the mechanism of gravitational baryogenesis. Aghamohammadi and Hossienkhani in [42] considered an anisotropic metric and investigated its effect on the baryon to entropy ratio in the context of $f(R)$ gravity. Odintsov et al in [43] studied gravitational baryogenesis in Loop quantum cosmology. This is the first instance where the mechanism of baryogenesis was investigated under the framework of a theory of quantized gravity. Baryogenesis was investigated in $f(T)$ gravity by Oikonomou et al in [44]. Gauss-Bonnett gravitational baryogenesis is studied in [45]. Recently in [46], Huang and Cai introduced gravitational baryogenesis mechanism in the vacuum inflation model and

showed that this model can produce acceptable baryon asymmetry. In [47], Sakstein and Solomon pointed out the importance of Lorentz-violating gravity theories that may yield matter-antimatter asymmetry consistent with the observational bound.

Drawing motivation from [43] we would like to investigate the gravitational baryogenesis mechanism in the framework of Hořava-Lifshitz gravity in this note. Section 2, is devoted to study the salient features of Hořava-Lifshitz gravity and baryogenesis in its framework. In this section, we also quantify the results and study the the values of the parameters for which the results can be compatible with the observational bounds. Section 3 is focussed to discuss the effect of scalar field on the gravitational baryogenesis in the framework of Hořava-Lifshitz gravity. In section 4 we will study baryogenesis with dark energy in the form generalized Chaplygin gas. Finally the paper ends with some concluding remarks in section 5.

2 Baryogenesis mechanism in the background of Hořava-Lifshitz Gravity

Here we consider a Friedmann-Robertson-Walker (FRW) background geometry with metric

$$ds^2 = c^2 dt^2 - d\sigma^2 = c^2 dt^2 - a^2 \left[\frac{dr^2}{1 - kr^2} + r^2 (d\theta^2 + \sin^2 \theta d\phi^2) \right] \quad (2.1)$$

where $a(t)$ is known as scale factor or expansion factor. Here the curvature, $k = -1, 0, 1$ represents open, flat and closed universe respectively.

Einstein's field equations for Hořava-Lifshitz gravity [48, 49] are given by

$$H^2 + \frac{k}{a^2} = \frac{8\pi G}{3} \rho + \frac{k^2}{2\Lambda a^4} + \frac{\Lambda}{2} \quad (2.2)$$

and

$$\dot{H} + \frac{3}{2}H^2 + \frac{k}{2a^2} = -4\pi G p - \frac{k^2}{4\Lambda a^4} + \frac{3\Lambda}{4} \quad (2.3)$$

where ρ and p are energy density and pressure of the universe, $H = \frac{\dot{a}}{a}$ is the Hubble parameter (choosing $c = 1$), Λ is the cosmological constant and G is the cosmological Newton's constant.

The energy density satisfies the continuity equation

$$\dot{\rho} + 3H(\rho + p) = 0 \quad (2.4)$$

From the above equation we get

$$\rho = \rho_0 a^{-3(1+\omega)} \quad (2.5)$$

where ρ_0 is the integration constant and $\omega = p/\rho$ is the EoS parameter.

The baryon-to-entropy ratio as given in [3] is

$$\frac{\eta_B}{s} \simeq -\frac{15g_b}{4\pi^2 g_*} \frac{\dot{R}}{M_*^2 T} \Big|_{T_D} \quad (2.6)$$

where g_b is the number of intrinsic degrees of freedom of the baryons, T_D is the critical temperature of the universe at which the baryon asymmetry generating interactions occur. g_* is the total degrees of freedom of effective massless particles ($g_* \sim 106$).

We shall assume that a thermal equilibrium exists and the universe evolves slowly from an equilibrium state to another equilibrium state. In this process the energy density is related to the temperature of each state by

$$\rho = \frac{\pi^2}{30} g_* T^4 \quad (2.7)$$

In the standard Einstein-Hilbert gravity framework, if the universe is filled with a perfect matter fluid with constant equation of state $\omega = p/\rho$, the Ricci scalar takes the form [45]

$$R = -8\pi G(1 - 3\omega)\rho \quad (2.8)$$

Using equations (2.2) and (2.3) the Ricci scalar reads

$$R = 8\pi G(1 - 3\omega)\rho + \frac{21\Lambda}{2} - \frac{6k}{a^2} \quad (2.9)$$

$$\dot{R} = 8\pi G(1 - 3\omega)\dot{\rho} + \frac{12k}{a^3}\dot{a} \quad (2.10)$$

Using the above result in equation (2.6), we obtain the baryon-to-entropy ratio for Hořava-Lifshitz gravity.

For a flat universe, Einstein's field equation (2.2) for Hořava-Lifshitz gravity can be analytically solved by using equation (2.5) to yield the scale factor

$$a(t) = \frac{16\pi}{3}^{\frac{1}{3(1+\omega)}} \left(\left(\frac{G\rho_0}{\Lambda} \right)^{\frac{1}{6}} \sinh \left[\frac{3}{4}(1+\omega)\sqrt{\Lambda}(\sqrt{2}t + 2\sqrt{3}C_1) \right]^{\frac{1}{3}} \right)^{\frac{2}{1+\omega}} \quad (2.11)$$

where C_1 is the integration constant. Correspondingly the Hubble's parameter takes the form

$$H(t) = \sqrt{\frac{\Lambda}{2}} \coth \left[\frac{3}{4}(1+\omega)\sqrt{\Lambda}(\sqrt{2}t + 2\sqrt{3}C_1) \right] \quad (2.12)$$

The energy density as a function of cosmic time is obtained as

$$\rho(t) = \frac{3\Lambda}{16\pi G} \left(\sinh \left[\frac{3}{4}(1+\omega)\sqrt{\Lambda}(\sqrt{2}t + 2\sqrt{3}C_1) \right]^{\frac{1}{3}} \right)^{-6} \quad (2.13)$$

Using equations (2.7) and (2.13) we obtain the decoupling time t_D as a function of critical temperature T_D as follows

$$t_D = \frac{2\sqrt{2}}{3(1+\omega)\sqrt{\Lambda}} \operatorname{arcsinh} \left[\frac{3}{2\pi} \sqrt{\frac{5\Lambda}{2\pi g_* G T_D^4}} \right] \quad (2.14)$$

By using equation (2.13) in equation (2.10) for flat universe, we get \dot{R} in terms of cosmic time as follows

$$\dot{R} = 2^{-\frac{3}{2}} 9(1+\omega)(3\omega - 1)\Lambda^{\frac{3}{2}} \coth \left[\frac{3}{4}(1+\omega)\sqrt{\Lambda}(\sqrt{2}t + 2\sqrt{3}C_1) \right] \times$$

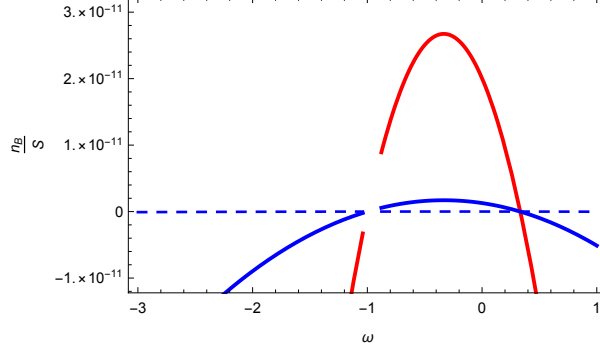


Fig.1

Figure 1: The baryon-to-entropy ratio η_B/s is plotted against the EOS parameter ω for $\Lambda = 10^{45.8}$ (dashed curve), $\Lambda = 10^{45.5}$ (red curve), $\Lambda = 10^{45.6}$ (blue curve). The parameters are considered as $-3 \leq \omega \leq 1.0$, $M_* = 10^{12} \text{ GeV}$, $T_D = 2 \times 10^{11}$, $g_b \simeq O(1)$, $g_* \simeq 106$ and $\rho_0 = 10^{102}$.

$$\left(\sinh \left[\frac{3}{4} (1 + \omega) \sqrt{\Lambda} (\sqrt{2}t + 2\sqrt{3}C_1) \right]^{\frac{1}{3}} \right)^{-6} \quad (2.15)$$

Using equation (2.14) the term \dot{R} in terms of decoupling temperature T_D takes the form

$$\begin{aligned} \dot{R} = 2^{-\frac{3}{2}} 9(1 + \omega)(3\omega - 1)\Lambda^{\frac{3}{2}} \coth \left(\operatorname{arcsinh} \left[\frac{3}{2\pi} \sqrt{\frac{5\Lambda}{2\pi g_* G T_D^4}} \right] \right) \times \\ \left(\sinh \left(\operatorname{arcsinh} \left[\frac{3}{2\pi} \sqrt{\frac{5\Lambda}{2\pi g_* G T_D^4}} \right] \right)^{\frac{1}{3}} \right)^{-6} \end{aligned} \quad (2.16)$$

Correspondingly by substituting \dot{R} from equation (2.16) in equation (2.6), the baryon-to-entropy ratio in the framework of Hořava-Lifshitz gravity is obtained as

$$\begin{aligned} \frac{\eta_B}{s} \simeq - \frac{135g_b(1 + \omega)(3\omega - 1)\Lambda^{\frac{3}{2}}}{8\sqrt{2}\pi^2 g_* M_*^2 T_D} \coth \left[\operatorname{arcsinh} \left(\frac{3}{2\pi} \sqrt{\frac{5\Lambda}{2\pi g_* G T_D^4}} \right) \right] \times \\ \left[\sinh \left(\operatorname{arcsinh} \left[\frac{3}{2\pi} \sqrt{\frac{5\Lambda}{2\pi g_* G T_D^4}} \right] \right)^{\frac{1}{3}} \right]^{-6} \end{aligned} \quad (2.17)$$

We proceed by investigating those circumstances under which the resulting baryon-to-entropy ratio can be compatible with the theoretical bound $\eta_B/s \leq 9 \times 10^{-11}$ [8]. Here we have assumed that the cutoff scale $M_* = 10^{12} \text{ GeV}$, $g_b \simeq O(1)$, the total number of the effectively massless particle in the universe $g_* \simeq 106$ [3, 4]. We also consider that $\rho_0 = 10^{102}$ and the decoupling temperature $T_D = 2 \times 10^{11}$. For these values we have drawn η_B/s as a function of equation of state parameter ω in figure 1 for three different values

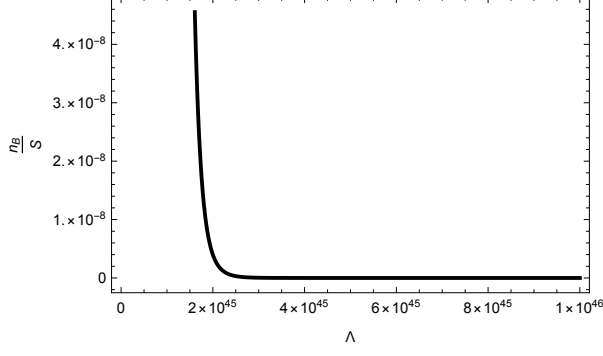


Fig.2(a)

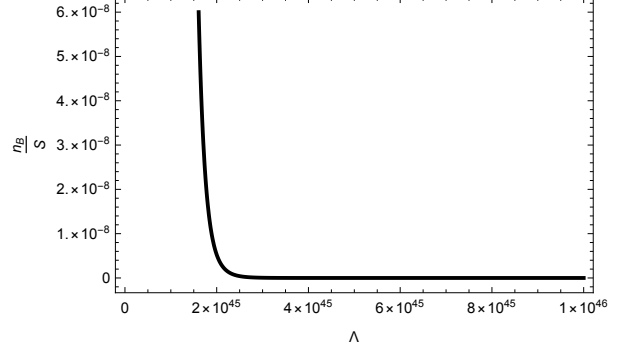


Fig.2(b)

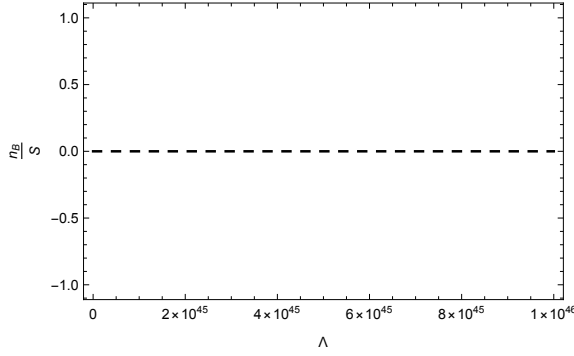


Fig.2(c)

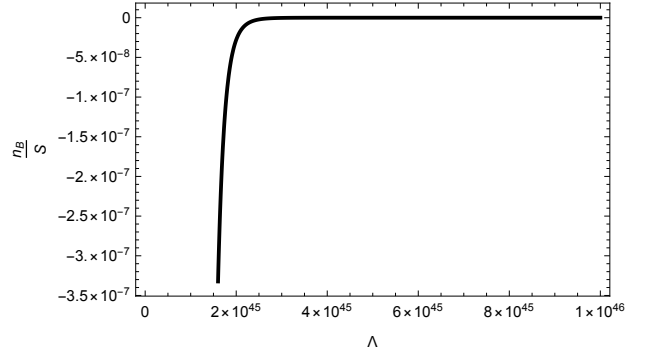


Fig.2(d)

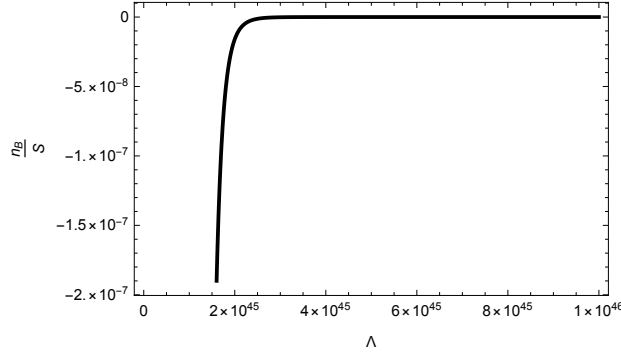


Fig.2(e)

Figure 2: The baryon-to-entropy ratio η_B/s is plotted against the parameter Λ for $\omega = 0$ (fig. 2(a)), $\omega = -0.3$ (fig. 2(b)), $\omega = 1/3$ (fig. 2(c)), $\omega = -2$ (fig. 2(d)) and $\omega = 1$ (fig. 2(e)). The parameters are considered as $M_* = 10^{12} \text{ GeV}$, $T_D = 2 \times 10^{11}$, $g_b \simeq \text{O}(1)$, $g_* \simeq 106$ and $\rho_0 = 10^{102}$.

of the parameter Λ . It can be seen that when $-1 < \omega < 0$, for $\Lambda = 10^{45.5}$ the resulting baryon-to-entropy ratio is $\eta_B/s \leq 2.5 \times 10^{-11}$ and for $\Lambda = 10^{45.6}$ ratio is $\eta_B/s \leq 2 \times 10^{-12}$, which are compatible with the observational bounds. But for $\omega < -1$, the ratio becomes

negative, therefore this case has no physical interest. The nature of baryon-to-entropy ratio also crucially depends on the model parameter Λ . In fig. 2 we have investigated the nature of η_B/s against Λ in different cosmological eras depending on the different values of the EOS parameter ω by choosing the previously stated values of the other parameters. The matter dominated era corresponds to $\omega = 0$. We can see from figure 2 that for $\omega = 0$, $\eta_B/s \leq 5 \times 10^{-8}$ and for $\omega = -0.3$, $\eta_B/s \leq 6 \times 10^{-8}$ and for both the cases baryon-to-entropy ratio decrease as Λ gets higher values. So, for the matter dominated era and for the epoch when the evolution of the universe is driven by quintessential fluid ($-1 < \omega < 0$), the baryon-to-entropy ratio gets the values that are in good agreement with the observationally accepted value. But for phantom region $\omega < -1$ and for $\omega = 1$ the results are physically unacceptable.

3 Baryogenesis with Scalar Field

Here we assume that the evolution of the universe is driven as usual, by a time-varying vacuum expectation value of some scalar field ϕ having energy density and pressure given by [21]

$$\rho(t) = V(\phi(t)) + \frac{1}{2}\dot{\phi}(t)^2 \quad (3.1)$$

and

$$p(t) = -V(\phi(t)) + \frac{1}{2}\dot{\phi}(t)^2 \quad (3.2)$$

where $V(\phi)$ is the effective potential of the field ϕ , the second term represents the kinetic contribution of ϕ . Here the ultra-relativistic particle contribution (radiation) has been neglected. It is assumed that the thermal corrections to the effective potential are negligible and that the scalar field has minimal coupling with the geometry [50]. We also assume

$$\phi(t) = \phi_0 t^n \quad \text{and} \quad V(\phi(t)) = V_0 \phi(t)^m \quad (3.3)$$

where $n > 1$ and m are positive constants. With this assumption (3.1) becomes

$$\rho(t) = \frac{1}{2}n^2 t^{2n-2} \phi_0^2 + V_0 t^{nm} \phi_0^m \quad (3.4)$$

Using equation (3.4) in equation (2.2) for flat universe we get the scale factor as

$$a(t) = C_2 \exp \left[t \sqrt{\frac{\Lambda}{2}} + \frac{4\pi G}{3\sqrt{2\Lambda}} \left(\frac{n^2 t^{2n-1} \phi_0^2}{2n-1} + \frac{2V_0 \phi_0^m t^{mn+1}}{1+mn} \right) \right] \quad (3.5)$$

where C_2 is an arbitrary integration constant. From equation (2.7) and equation (3.4) we have obtained the relation between decoupling time t_D and critical temperature T_D for $m = 1$ and $n = 2$ as

$$t_D = \frac{\sqrt{g}\pi T_D^2}{\sqrt{30\phi_0(V_0 + 2\phi_0)}} \quad (3.6)$$

Using equation (3.5) for $m = 1$, $n = 2$ in (2.10) we get \dot{R} for flat universe

$$\dot{R} = 16\pi G t \phi_0 (1 - 3\omega)(V_0 + 2\phi_0) \quad (3.7)$$

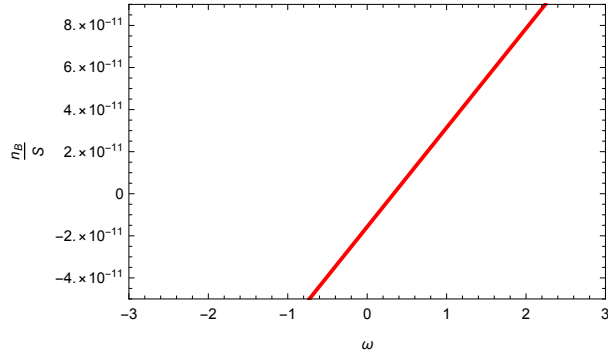


Fig.3

Figure 3: The baryon - to - entropy ratio η_B/s for scalar field is plotted against the EOS parameter ω . The parameters are considered as $-3 \leq \omega \leq 3$, $M_* = 10^{12} \text{ GeV}$, $T_D = 2 \times 10^{16}$, $g_b \simeq \text{O}(1)$, $g_* \simeq 106$, $\phi_0 = 10^7$ and $V_0 = 10^5$.

Exploiting equation (3.6), (3.7) becomes

$$\dot{R} = 8\sqrt{\frac{2g}{15}}\pi^2 GT_D^2(3\omega - 1)\sqrt{\phi_0(V_0 + 2\phi_0)} \quad (3.8)$$

With the help of equations (3.8) and (2.6) the baryon-to entropy ratio in this scenario reads

$$\frac{\eta_B}{s} \simeq \frac{2\sqrt{30}Gg_b T_D(1 - 3\omega)\sqrt{\phi_0(V_0 + 2\phi_0)}}{\sqrt{g}M^2} \quad (3.9)$$

In figure 3 we have investigated the profile of baryon to entropy ratio for scalar field against the EOS parameter ω for $\phi_0 = 10^7$ and $V_0 = 10^5$. In this scenario we have found $\eta_B/s \leq 8 \times 10^{-11}$. In figure 4(a) and figure 4(b) we have plotted the behavior of the baryon-to-entropy ratio for scalar field as a function of ϕ_0 for $T_D = 2 \times 10^{11}$ and $T_D = 2 \times 10^{16}$ respectively with the previously described values of the parameters M_* , g_b , g_* and $V_0 = 10^{10}$. It is observed that η_B/s takes observationally accepted value as the decoupling temperature T_D attains lower values. For $T_D = 2 \times 10^{11}$ the baryon-to entropy ratio becomes $\eta_B/s \leq 4.5 \times 10^{-8}$. But for $T_D = 2 \times 10^{16}$, the baryon-to entropy ratio gets value $\eta_B/s \leq 4 \times 10^{-3}$ which is far from the observational bound. In each case, η_B/s increases as ϕ_0 increases for $\omega = 1$. In figure 5(a) and 5(b) we have plotted η_B/s for scalar field as a function of V_0 for $T_D = 2 \times 10^{11}$ and $T_D = 2 \times 10^{16}$ respectively and have find that η_B/s increases as V_0 increases for $\omega = 1$. In this era, the baryon-to entropy ratio becomes $\eta_B/s \leq 3 \times 10^{-12}$ for $T_D = 2 \times 10^{11}$ and $\eta_B/s \leq 3 \times 10^{-7}$ for $T_D = 2 \times 10^{16}$. For the other values of ω we get un-physical results.

4 Baryogenesis with Generalized Chaplygin Gas

As discussed earlier the energy density of Generalized Chaplygin Gas (GCG) [36] is given by $p_{GCG} = -\frac{A}{\rho_{GCG}^\alpha}$, where $0 < \alpha \leq 1$ and A is a positive constant. In the framework of

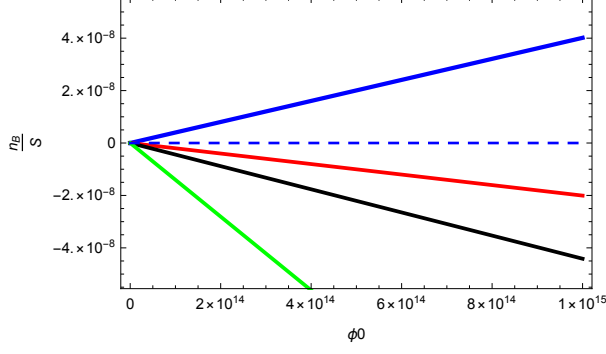


Fig.4(a)

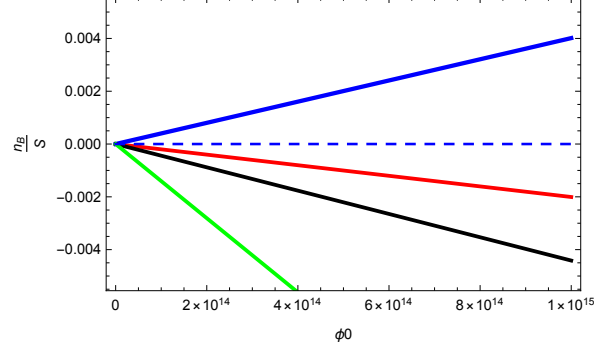


Fig.4(b)

Figure 4: The baryon-to-entropy ratio η_B/s for scalar field is plotted against the parameter ϕ_0 for $\omega = -2$ (green curve), $\omega = -0.4$ (black curve), $\omega = 0$ (red curve), $\omega = 1/3$ (dashed blue curve) and $\omega = 1$ (blue curve). The parameters are considered as $M_* = 10^{12} \text{ GeV}$, $g_b \simeq \text{O}(1)$, $g_* \simeq 106$ and $V_0 = 10^{10}$. The left plot corresponds to $T_D = 2 \times 10^{11}$ while the right plot corresponds to $T_D = 2 \times 10^{16}$.

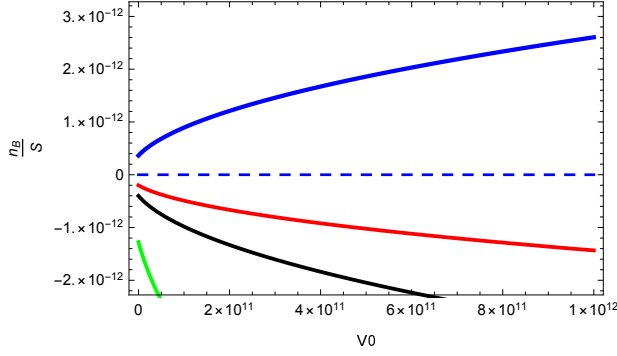


Fig.5(a)

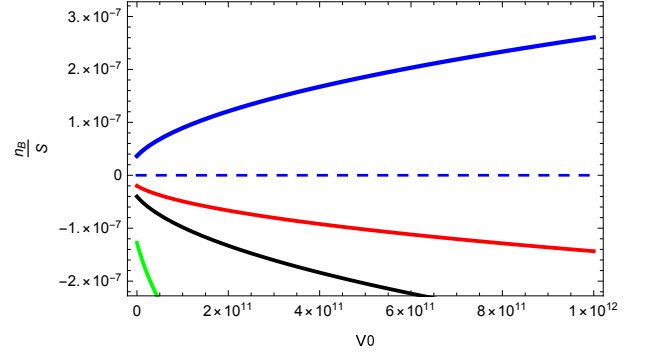


Fig.5(b)

Figure 5: The baryon-to-entropy ratio η_B/s for scalar field is plotted against the parameter V_0 for $\omega = -2$ (green curve), $\omega = -0.4$ (black curve), $\omega = 0$ (red curve), $\omega = 1/3$ (dashed blue curve) and $\omega = 1$ (blue curve). The parameters are considered as $M_* = 10^{12} \text{ GeV}$, $g_b \simeq \text{O}(1)$, $g_* \simeq 106$ and $\phi_0 = 10^{10}$. The left plot corresponds to $T_D = 2 \times 10^{11}$ while the right plot corresponds to $T_D = 2 \times 10^{16}$.

FRW cosmology, with the energy conservation equation it leads to

$$\rho_{GCG} = \left(A + B a^{-3(1+\alpha)} \right)^{\frac{1}{1+\alpha}} \quad (4.1)$$

where $0 < \alpha \leq 1$, A is a positive constant and B is a positive integration constant. Using equation (2.2) and (4.1) we obtain the scale factor for a flat universe as follows

$$a(t) = \left[\frac{e^{\frac{(1+\alpha)}{2\sqrt{\Lambda}}(3\Lambda+8G\pi A^{\frac{1}{1+\alpha}})(\sqrt{2}t+6\sqrt{\Lambda}C_3(1+\alpha))} - 8\pi GB}{(1+\alpha)(3\Lambda + 8G\pi A^{\frac{1}{1+\alpha}})} \right]^{\frac{1}{3(1+\alpha)}} \quad (4.2)$$

where C_3 is an integration constant. The above choice of scale factor yields the Hubble parameter as

$$H(t) = \left[\frac{(3\Lambda + 8G\pi A^{\frac{1}{1+\alpha}})e^{\frac{(1+\alpha)}{2\sqrt{\Lambda}}(3\Lambda+8G\pi A^{\frac{1}{1+\alpha}})(\sqrt{2}t+6\sqrt{\Lambda}C_3(1+\alpha))}}{3\sqrt{2\Lambda} \left(e^{\frac{(1+\alpha)}{2\sqrt{\Lambda}}(3\Lambda+8G\pi A^{\frac{1}{1+\alpha}})(\sqrt{2}t+6\sqrt{\Lambda}C_3(1+\alpha))} - 8\pi GB \right)} \right] \quad (4.3)$$

Correspondingly the energy density in terms of cosmic time becomes

$$\rho_{GCG}(t) = \left(A + \frac{B(1+\alpha)(3\Lambda + 8G\pi A^{\frac{1}{1+\alpha}})}{e^{\frac{(1+\alpha)}{2\sqrt{\Lambda}}(3\Lambda+8G\pi A^{\frac{1}{1+\alpha}})(\sqrt{2}t+6\sqrt{\Lambda}C_3(1+\alpha))} - 8\pi GB} \right)^{\frac{1}{1+\alpha}} \quad (4.4)$$

Combining equations (4.4) and (2.7) we get the relation between decoupling time t_D and critical temperature T_D in this scenario, which is given by

$$t_D = \frac{B}{\sqrt{2}(1+\alpha)(3\Lambda + 8G\pi A^{\frac{1}{1+\alpha}})} \left[8\pi G + \frac{(1+\alpha)30^{(1+\alpha)}(3\Lambda + 8G\pi A^{\frac{1}{1+\alpha}})}{\pi^{2(1+\alpha)}g^{(1+\alpha)}T_D^{4(1+\alpha)} - 30^{(1+\alpha)}A} \right] - 6(1+\alpha)C_3\sqrt{\frac{\Lambda}{2}} \quad (4.5)$$

From equations (4.4) and (2.10) we get

$$\begin{aligned} \dot{R} = & -4\sqrt{\frac{2}{\Lambda}}G\pi B(1-3\omega)(1+\alpha)e^{\frac{(1+\alpha)}{2\sqrt{\Lambda}}(3\Lambda+8G\pi A^{\frac{1}{1+\alpha}})(\sqrt{2}t+6\sqrt{\Lambda}C_3(1+\alpha))} \times \\ & (3\Lambda + 8G\pi A^{\frac{1}{1+\alpha}})^2 \left(e^{\frac{(1+\alpha)}{2\sqrt{\Lambda}}(3\Lambda+8G\pi A^{\frac{1}{1+\alpha}})(\sqrt{2}t+6\sqrt{\Lambda}C_3(1+\alpha))} - 8\pi GB \right)^{-2} \times \\ & \left(A + \frac{B(1+\alpha)(3\Lambda + 8G\pi A^{\frac{1}{1+\alpha}})}{e^{\frac{(1+\alpha)}{2\sqrt{\Lambda}}(3\Lambda+8G\pi A^{\frac{1}{1+\alpha}})(\sqrt{2}t+6\sqrt{\Lambda}C_3(1+\alpha))} - 8\pi GB} \right)^{-1+\frac{1}{1+\alpha}} \end{aligned} \quad (4.6)$$

Again using equation (4.5) the above form of \dot{R} is expressed in terms of T_D

$$\dot{R} = -4\sqrt{\frac{2}{\Lambda}}G\pi B(1-3\omega)(1+\alpha)e^{\frac{B}{\sqrt{\Lambda}} \left(4\pi G + \frac{2^\alpha 15^{(1+\alpha)}(1+\alpha)(3\Lambda+8G\pi A^{\frac{1}{1+\alpha}})}{g^{(1+\alpha)}\pi^{2(1+\alpha)}T_D^{4(1+\alpha)} - A30^{(1+\alpha)}} \right)} \times$$

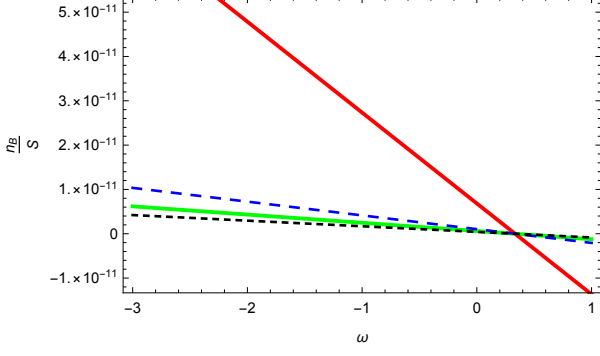


Fig.6(a)

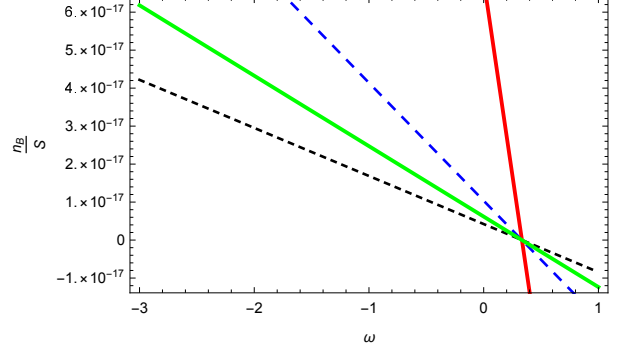


Fig.6(b)

Figure 6: The baryon - to - entropy ratio η_B/s for GCG is plotted against the EOS parameter ω for $\alpha = 0.8$ (red curve), $\alpha = 0.93$ (dashed blue curve), $\alpha = 1$ (dashed black curve), $\alpha = 0.97$ (green curve). The parameters are considered as $-3 \leq \omega \leq 1.0$, $M_* = 10^{12} \text{ GeV}$, $g_b \simeq O(1)$, $g_* \simeq 106$, $A = 5.5 \times 10^{10}$ and $B = 9 \times 10^{-25}$. Fig. 6(a) corresponds to $T_D = 2 \times 10^{11}$ and Fig. 6(b) corresponds to $T_D = 2 \times 10^{16}$

$$(3\Lambda + 8G\pi A^{\frac{1}{1+\alpha}})^2 \left(e^{\frac{B}{\sqrt{\Lambda}} \left(4\pi G + \frac{2^\alpha 15^{(1+\alpha)} (1+\alpha) (3\Lambda + 8G\pi A^{\frac{1}{1+\alpha}})}{g^{(1+\alpha)} \pi^{2(1+\alpha)} T_D^{4(1+\alpha)} - A_{30(1+\alpha)}} \right)} - 8\pi GB \right)^{-2} \times$$

$$\left(A + \frac{B(1+\alpha)(3\Lambda + 8G\pi A^{\frac{1}{1+\alpha}})}{e^{\frac{B}{\sqrt{\Lambda}} \left(4\pi G + \frac{2^\alpha 15^{(1+\alpha)} (1+\alpha) (3\Lambda + 8G\pi A^{\frac{1}{1+\alpha}})}{g^{(1+\alpha)} \pi^{2(1+\alpha)} T_D^{4(1+\alpha)} - A_{30(1+\alpha)}} \right)} - 8\pi GB} \right)^{-1 + \frac{1}{1+\alpha}} \quad (4.7)$$

Inserting equation (4.7) into (2.6) the baryon-to entropy reads

$$\frac{\eta_B}{s} \simeq \frac{15\sqrt{2}BGg_b(1-3\omega)(1+\alpha)}{\pi g T_D M_* \sqrt{\Lambda}} e^{\frac{B}{\sqrt{\Lambda}} \left(4\pi G + \frac{2^\alpha 15^{(1+\alpha)} (1+\alpha) (3\Lambda + 8G\pi A^{\frac{1}{1+\alpha}})}{g^{(1+\alpha)} \pi^{2(1+\alpha)} T_D^{4(1+\alpha)} - A_{30(1+\alpha)}} \right)} \times$$

$$(3\Lambda + 8G\pi A^{\frac{1}{1+\alpha}})^2 \left(e^{\frac{B}{\sqrt{\Lambda}} \left(4\pi G + \frac{2^\alpha 15^{(1+\alpha)} (1+\alpha) (3\Lambda + 8G\pi A^{\frac{1}{1+\alpha}})}{g^{(1+\alpha)} \pi^{2(1+\alpha)} T_D^{4(1+\alpha)} - A_{30(1+\alpha)}} \right)} - 8\pi GB \right)^{-2} \times$$

$$\left(A + \frac{B(1+\alpha)(3\Lambda + 8G\pi A^{\frac{1}{1+\alpha}})}{e^{\frac{B}{\sqrt{\Lambda}} \left(4\pi G + \frac{2^\alpha 15^{(1+\alpha)} (1+\alpha) (3\Lambda + 8G\pi A^{\frac{1}{1+\alpha}})}{g^{(1+\alpha)} \pi^{2(1+\alpha)} T_D^{4(1+\alpha)} - A_{30(1+\alpha)}} \right)} - 8\pi GB} \right)^{-1 + \frac{1}{1+\alpha}} \quad (4.8)$$

By choosing $M_* = 10^{12} \text{ GeV}$, $g_b \simeq O(1)$, $g_* \simeq 106$, $A = 5.5 \times 10^{10}$ and $B = 9 \times 10^{-25}$ we have plotted the functional dependence of baryon-to-entropy ratio as a function of

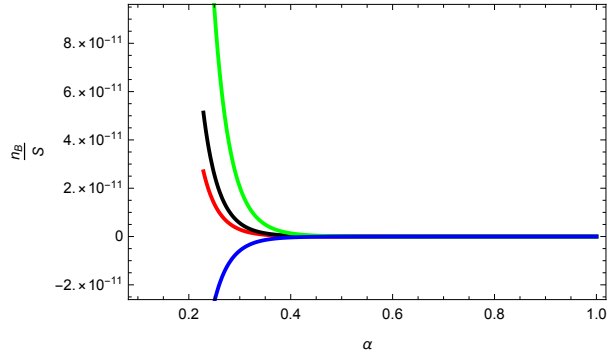


Fig.7

Figure 7: The baryon-to-entropy ratio η_B/s for GCG is plotted against the GCG model parameter α for $\omega = -2$ (green curve), $\omega = -0.3$ (black curve), $\omega = 0$ (red curve) and $\omega = 1$ (blue curve). The parameters are considered as $M_* = 10^{12} \text{ GeV}$, $T_D = 2 \times 10^{16}$, $g_b \simeq \mathcal{O}(1)$, $g_* \simeq 106$, $A = 5.5 \times 10^{10}$, $B = 9 \times 10^{-25}$ and $\Lambda = 10^{45.5}$.

EOS parameter ω in figure 6 for four different values of the GCG parameter α . It can be seen that corresponding to $T_D = 2 \times 10^{11}$, baryon-to-entropy ratio predicted by (4.8) is $\eta_B/s \leq 8.5 \times 10^{-11}$ for $\alpha = 0.8$, which is very close to observationally accepted value. Whereas the predicted value of baryon-to-entropy ratio corresponding to $T_D = 2 \times 10^{16}$ is $\eta_B/s \leq 7 \times 10^{-16}$ for $\alpha = 0.8$. It is also observed that as α takes higher values between $0.8 < \alpha < 1$ the ratio assumes smaller values compared to the observed value. Thus the model parameter α affects the ratio in a crucial way. Next in figure 7, we have investigated the nature of the baryon-to-entropy ratio as a function of GCG parameter α in various phase of the evolution of the universe. It can be seen that in the matter dominated era, for quintessential fluid and for phantom dark energy baryon-to-entropy ratio takes positive values and η_B/s decreases as α increases. But for $\omega = 1$, η_B/s shows un-physical result.

5 Conclusion

Here we have investigated the gravitational baryogenesis mechanism under the framework of Hořava-Lifshitz gravity. The baryon-to-entropy ratio is computed for Hořava-Lifshitz gravity in terms of scale factor and finally in terms of the decoupling temperature.

In contrary to the other works done on the gravitational baryogenesis [4, 43, 45], our computed Baryon-to-entropy ratio in the framework of Hořava-Lifshitz gravity is independent of the critical density parameter ρ_0 . Baryon-to-entropy ratio have been generated against the EOS parameter ω and the model parameter Λ . We have seen that these parameters play a crucial role to make the value compatible with the observational bound. It should be noted that to make the considered scenario viable, we have assumed the decoupling temperature $T_D = 2 \times 10^{11}$. With this assumption we have observed that if the expansion of the universe is driven by quintessential fluid the ratio becomes consistent with the observational bounds for $\Lambda = 10^{45.5}$ and $\Lambda = 10^{45.6}$. Also in case of matter dominated

universe we have seen that the ratio gets values compatible with the observational data for these two values of Λ . But when the evolution of the universe is dominated by phantom like dark energy, we get un-physical results. In the radiation dominated epoch ($\omega = 1/3$) the baryon-to-entropy ratio becomes zero like Einstein-Hilbert case. In the early universe prior to radiation dominated epoch ($\omega > 1/3$) we get un-physical results.

Further we have investigated the baryogenesis mechanism for a scalar field in the context of Hořava-Lifshitz gravity. We have chosen the scalar field and the scalar potential in the power-law form and have computed the scale factor in a general case. Then we have investigated the mechanism for particular values of the power-law parameters. For this selection, we have studied the behavior of the baryon-to-entropy ratio as a function of EoS parameter ω for $T_D = 2 \times 10^{16}$. We have seen that the ratio η_B/s always increases as ω increases and attains value that is very near to observational bound. Again η_B/s is plotted against the model parameters ϕ_0 and V_0 for different values of EOS parameter ω . In both the cases, we have found results compatible with observational data only for $\omega = 1$. We get un-physical results for the other values of ω . We have compared the results for $T_D = 2 \times 10^{11}$ and for $T_D = 2 \times 10^{16}$ and found that as T_D gets lower values, η_B/s gets closer to the observational bound.

Next we have investigated the effect of a unified dark fluid model GCG on the process of baryogenesis in the framework of Hořava-Lifshitz gravity. We have observed that the resulting baryon-to entropy significantly depends on the GCG model parameters. It is observed that for $0.8 \leq \alpha \leq 1$ and $T_D = 2 \times 10^{11}$ the ratio gets values that are very close to the observational bound. η_B/s always decreases as ω increases. In this scenario for $\omega < -1$, $-1 < \omega < 0$ and $\omega = 0$, the values of η_B/s are in very good agreement with observation, but $\omega < -1$ shows un-physical result. Finally it must be stated that the quantum mechanical nature of the background geometry of Hořava-Lifshitz gravity plays an active role in the observations obtained in this study.

Acknowledgements

PR acknowledges University Grants Commission (UGC), Government of India for providing research project grant (No. F.PSW-061/15-16 (ERO)). PR also acknowledges Inter University Centre for Astronomy and Astrophysics (IUCAA), Pune, India, for awarding Visiting Associateship.

References

- [1] Bennet, C. L. et al., [WMAP Collaboration] *Astrophys. J. Suppl.* **148** 1 (2003)
- [2] Burles, S., Nollett, K. M., and Turner, M. S., *Phys. Rev. D* **63**, 063512 (2001).
- [3] Davoudiasl, H., Kitano, R., Kribs, G. D., Murayama, H. and Steinhardt, P. J., *Phys. Rev. Lett.* **93** 201301 (2004).
- [4] Lambiase, G. and Scarpetta, G., *Phys. Rev. D* **74**, 087504 (2006).
- [5] Lambiase, G., *Phys. Lett. B* **642**, 9 (2006).

- [6] Li, H., Li, M. Z., and Zhang, X. M., *Phys. Rev. D* **70**, 047302 (2004).
- [7] Sakharov, A. D., *Pisma Zh. Eksp. Teor. Fiz.* **5**, 32 (1967)[JETP Lett. 5, 24 (1967)] [Sov. Phys. Usp. 34, 392 (1991)] [Usp.Fiz. Nauk 161, 61 (1991)].
- [8] Bennet, C. L. et al.,*Ap. J. Suppl. Ser.* **148** 15 (2003).
- [9] Perlmutter, S. et al., *Astrophys. J.* **517** 565 (1999).
- [10] Spergel, D. N. et al., *Astron. J. Suppl.* **148** 175 (2003).
- [11] Horava, P., *Phys. Rev. D* **79** 084008 (2009).
- [12] Horava, P., *JHEP* **0903** 020 (2009).
- [13] Horava, P., *Phys. Rev. Lett.* **102** 161301 (2009).
- [14] Stelle, K. S., *Phys. Rev. D* **16** 953 (1977).
- [15] Biswas, T., Gerwick, E., Koivisto, T., and Mazumdar, A., *Phys. Rev. Lett.* **108** 031101 (2012).
- [16] Khodadi, M. et. al., *Phys. Rev. D.* **93** 124019 (2016).
- [17] Hartong, J., Obers, N. A., *JHEP* **1507** 155 (2015).
- [18] Garattini, R., Saridakis, E. N., *Eur. Phys. J. C.* **75** 343 (2015).
- [19] Ranjit, C., Rudra, P., *Int. J. Theor. Phys.* **55** 636 (2016).
- [20] Rudra, P., Debnath, U., *Int. J. Theor. Phys.* **53** 2668 (2014).
- [21] Lucchin, F., Matarrese, S., *Phys. Rev. D* **32** 6 (1985).
- [22] Bamba, K., Capozziello, S., Nojiri, S., Odintsov, S. D., *Astrophys. Space Sci.* **342** 155 (2012).
- [23] Ratra, B., Peebles, P. J. E., *Phys. Rev. D* **37** 3406 (1988).
- [24] Bamba, K., Razina, O., Yerzhanov, K., Myrzakulov, R., *Int. J. Mod. Phys. D* **22** 1350023 (2013).
- [25] Gorini, V., Kamenshchik, A. Y., Moschella, U., Pasquier, V., *Phys. Rev. D* **69** 123512 (2004).
- [26] Wei, H., Cai, R.-G., Zeng, D.-F., *Class. Quant. Grav.* **22** 3189 (2005).
- [27] Kamenshchik, A. Y., Moschella, U., Pasquier, V., *Phys. Lett. B* **511** 265 (2001).
- [28] Bento, M. C., Bertolami, O., Sen, A. A. *Phys. Rev.* **66** 043507(2002).
- [29] Dinda, B. R., Kumar, S., Sen, A. A., *Phys. Rev. D.* **90** no.8, 083515 (2014).
- [30] del Campo, S., Fadrakas, C. R., Herrera, R., Leiva, C., Leon, G., Saavedra, J., *Phys. Rev. D.* **88** (2013) 023532.
- [31] Setare, M. R., *Eur. Phys. J. C.* **52** (2007) 689-692.
- [32] Setare, M. R., *Phys. Lett. B* **654** (2007) 1-6.
- [33] Lopez, M. B., Gonzalez-Diaz, P. F., Martin-Moruno, P., *Int.J.Mod.Phys. D* **17** (2008) 2269-2290.
- [34] Bertolami, O., Silva, P. T., *Mon.Not.Roy.Astron.Soc.* **365** (2006) 1149-1159.
- [35] Billic, N., Tupper, G. B. and Viollier, R. D., *Phys. Lett. B* **535** 17 (2001).
- [36] Bento, M. C., Bertolami, o. and Sen, A. A., *arXiv: 0202064v2* [gr-qc] (2002).

- [37] Xu, L. and Lu, J. *JCAP* **025** 1003 (2010).
- [38] Lu, J., Gui, Y., Xu, L., *Eur. Phys. J. C* **63** 349 (2009).
- [39] Li, Z., Wu, P. and Yu, H., *JCAP* **017** 09 (2009).
- [40] Wu, P. and Yu, H., *Phys. Lett. B* **16** 644 (2007).
- [41] Ramos, M. P. L. P and Paramos, J., *arXiv: 1709.04442v1* [gr-qc] (2017).
- [42] Aghamohammadi, A. and Hossienkhani, H., *arXiv: 1709.06996v1* [physics.gen-ph] (2017).
- [43] Odintsov, S. D. and Oikonomou, V. K., *Europhys. Lett.* **116** 4 (2016).
- [44] Oikonomou, V. K. and Saridakis, E. N., *Phys. Rev. D* **94** 124005 (2016).
- [45] Odintsov, S. D. and Oikonomou, V. K., *Phys. Lett. B* **760** 259 (2016).
- [46] Huang, Z. and Cai, Q., *arXiv: 1708.09137v1* [gr-qc] (2017).
- [47] Sakstein, J. and Solomon, A. R., *Phys. Lett. B* **773** 186-190 (2017).
- [48] Bhattacharya, S. and Debnath, U., *Int. J. Mod. Phys. D*, **20** 1191 (2011).
- [49] Jamil, M. and Saridakis, E. N., *JCAP* **07** 028 (2010).
- [50] Linde, A. D. *Rep. Prog. Phys.* **47** 925 (1984).